Polymer Journal, Vol. 26, No. 4, pp 439—463 (1994)

Thermodynamics of Formation of Porous Polymeric Membrane by Phase Separation Method III. Pore Formation by Contacting Secondary Particles: Theory and Its Comparison with Experiments

Hideki IIJIMA, Shigenobu MATSUDA, and Kenji KAMIDE*

Fundamental Research Laboratory of Natural & Synthetic Polymers, Asahi Chemical Industry Co., Ltd., 11-7 Hacchonawate, Takatsuki, Osaka 569, Japan
**Laboratory of Clothing, Faculty of Education, Kumamoto University, Kurokami 2-40-1, Kumamoto 860, Japan*

(Received August 2, 1993)

ABSTRACT: An attempt was made (1) to establish a theory of pore characteristics, including pore size distribution $N(r)$ (r, radius of pore) for porous polymeric membranes, prepared by the phase separation method, using two-phase volume ratio R ($\equiv V_{(1)}/V_{(2)}$; $V_{(1)}$ and $V_{(2)}$ are volumes of polymer-lean and -rich phases, respectively) and radius of secondary particle S_2 and (2) to compare the $N(r)$ calculated from R and S_2 with that by an electron micrographic (EM) method. For this purpose, we assume that secondary particles (*i.e.*, polymer-rich phase) and hypothetical vacant particles (*i.e.*, polymer-lean phase) are placed randomly on a hexagonal closest packing lattice and that x vacant particles contact with each other to form a pore (referred to as vacant-particle pore). An expression of the probability $P(x)$ that a given pore contains x vacant particles was derived. With consideration of an increase in pore size after drying, $N(r)$ for vacant-particle pores, $N_v(r)$ was derived, using R, S_2 and pore density of vacant-particle pores N_P (number/m^2), and by translating x to pore radius r. The condition of determining N_P from R and S_2 was established. $N(r)$ for inter-polymer-particle pores, $N_i(r)$ (*i.e.*, crevasses of closest-packed secondary particles) was also calculated by using R and S_2. The theory predicts that smaller pore size can be attained with smaller R and S_2. Phase volume ratio R was found to be determined through use of a theoretical equation on porosity, using experimental porosity $Pr(d_4)$ determined from electron micrographs and approximate of degree of collapse of a membrane $k'(=L_0/L_d$; L_0, thickness of cast solution; L_d, that of dried membrane). Collapse of a hypothetical gel membrane during coagulation process explains well the findings that theoretical $N(r)$ coincides fairly well with that by EM method only when apparent phase volume ratio R_A is employed instead of R.

KEY WORDS Particle Growth Concept / Phase Separation / Porous Polymeric Membrane / Pore Size Distribution / Hexagonal Lattice / Secondary Particle / Vacant Particle / Cellulose Cuprammonium Solution / Collapse /

In the previous papers,[1,2] we proposed a theory of nucleation (steps a and b in Figure 1), growth of nuclei to the primary particles (steps b—d in Figure 1), and growth of the primary particles to the secondary particles (steps d—f in Figure 1) in the process of formation of the porous polymeric membranes by the phase separation method (*i.e.*, solvent-casting method) in the case when initial polymer volume fraction v_p^0 is less than the polymer volume fraction at a critical solution point v_p^c. In subsequent steps, the secondary particles contact with each other to form gel membranes, which become dried membrane through desolvation and drying (steps g—j in Figure 1).

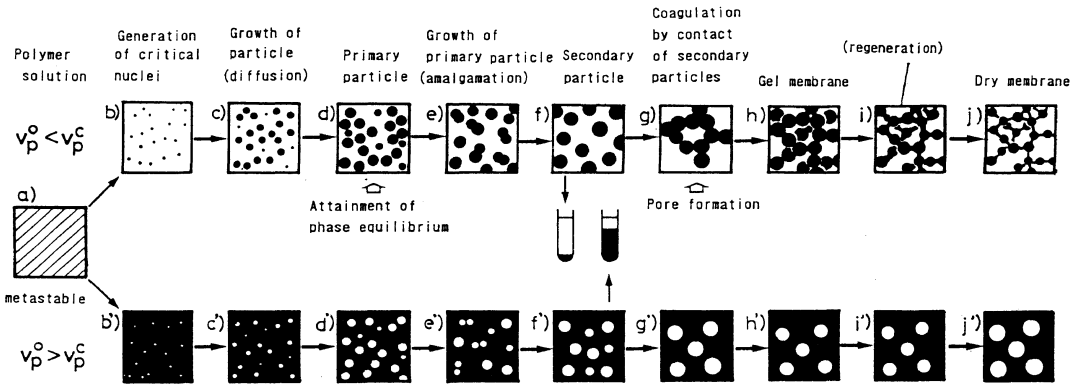

Figure 1. Elementary steps in porous polymeric membrane formation by the phase separation method: v_p^0, polymer volume fraction of the solution when the phase separation occurs; v_p^c, polymer volume fraction of critical solution point; steps a and f—j correspond to those of a and f—j in Figure 10, respectively.

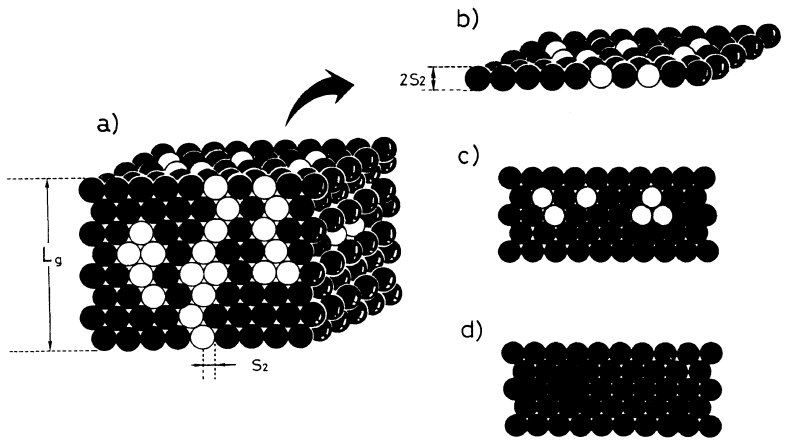

Figure 2. Schematic representation of a membrane structure and pores: a), A multi-layer model of a membrane; filled sphere, polymer particle; unfilled sphere, vacant particle; diameter of these spheres are $2S_2$; b), A hypothetical plane; c) Vacant-particle pores on a hexagonal closest packing lattice; d) Inter-polymer-particle pores brought about by contacted polymer particles.

Based on electron microscopic observation of membranes prepared by the solvent-casting method, Kamide *et al.* proposed "particle growth concept" on membrane formation mechanism in the phase separation method (Figure 1)[3,4] and "two-dimensional thin layer model" of membrane surface (Figure 2b)[4] which consists of the secondary particles of polymer-rich phase (referred to as "polymer particles") with radii of S_2 and hypothetical particles of polymer-lean phase (referred to as "vacant particles"), whose radii are also S_2. In the thin layer model, regarding a portion consisting of contacting vacant particles as pores, whose boundary should be fully surrounded by polymer particles (Figure 2c; we define these pores as "vacant-particle pores"), Kamide and Manabe (KM)[4] attempted to derive an tentative equation of pore radius distribution $N(r)$ (r, radius of pore) of membranes as a function of S_2 and two phase volume ratio at the instant when phase separation occurs R ($\equiv V_{(1)}/V_{(2)}$; $V_{(1)}$ and $V_{(2)}$ are volumes of polymer-lean and -rich phases,

respectively), which is indirectly calculated from porosity *Pr* of a membrane evaluated by an electron micrographic (EM) method.[5]

Unfortunately, $N(r)$ of KM theory contains the following unnegligible drawbacks: a) In calculation of probability of appearance of the vacant-particle pore with x vacant particles $P(x)$, a portion which does not contain any vacant particle (*i.e.*, $x=0$) is mistakenly considered as a vacant-particle pore. Furthermore, $P(x)$ was normalized over the range of $x=0$ to $x=N_T L$. Here, N_T is a total number of both particles (polymer- and vacant-particles) in the unit area of the plane (see, eq 1) and L is volume fraction of polymer-lean phase (see, eq 2). Accordingly, the final equation of $N(r)$ can not ascertain the existence of N_P vacant-particle pores in unit area by KM theory. b) They thought that R could be indirectly determined from *Pr* by EM method, however, R thus calculated often deviates significantly from R directly determined in actual phase separation experiments. c) Even if $x=0$, small crevasses are formed between closely-packed polymer particles and these crevasses should be regarded as pores, which we define as inter-polymer-particle pores, but these crevasses were not considered in KM theory. These inter-polymer-particle pores must be taken into consideration independently. d) Pore density N_P can not be determined explicitly for a given condition of R and S_2.

Recently, Kamide *et al.*[6] disclosed for membranes by the phase separation method that the over-all supermolecular structure changed significantly depending on the distance from the top surface of a membrane and within a given thin layer with the constant distance from the surface, the particular supermolecular structure of the layer remained almost uniform, and that $N(r)$ for each portion of the ultra-thin layer was constant for a given distance. These experimental facts leaded them to the conclusion that porous polymeric membrane prepared by the phase separation method should be considered as a composite, in which many hypothetical ultra-thin layers are piled up, and they presented a "three-dimensional structure model" of a membrane, assuming that the over-all supermolecular structure is uniform (Figure 2a).[7]

In this article, we attempted (1) to derive a reliable equation of $N(r)$ for vacant-particle pores of a thin layer using R and S_2 (eq 24) by improving the drawback a) of the previous KM theory, (2) to interpret the experimental disagreement between two kinds of R; the one is calculated indirectly from *Pr* evaluated by EM method and the other is directly determined in actual phase separation experiments [drawback b) in KM theory], by considering collapse (steps g—h in Figure 1) of gel membranes, with the three-dimensional model of a membrane (Figure 2a), proposing a new concept of apparent phase volume ratio R_A (eq 39), (3) to derive equations for pore density of inter-polymer-particle pores and pore size distribution of them using R and S_2 (eq 31 and 34, respectively) [drawback c)], and (4) to give concrete physical meanings of determining N_P value from the boundary condition [drawback d)], demonstrating effects of R and S_2 on $N(r)$.

THEORETICAL BACKGROUND

Lattice Theory for Vacant-Particle Pore

Pore Radius Distribution. After the growing particles approached their asymptotic size (*i.e.*, the secondary particle; step f in Figure 1), the particles contact with each other forming pores by settling the coagulated solution without any further agitation (step g in Figure 1).

Assume that a membrane consists of multi-layers (see, Figure 2a) and that the pore characteristics of a hypothetical plane within the membrane, parallel to the membrane surface is kept the same.[6] Consider a hypothetical plane with thickness $2S_2$, parallel to the surface of the coagulated solution and assume that the solution consists of the polymer particles with radius of S_2 and "hypothetical particles" of

polymer-lean phase, whose radius is also S_2 (see, Figure 2b). Let the number of the polymer particles per unit area of the plane be represented by $N_T/(R+1)$ and that of the hypothetical polymer-lean particles (referred to as "vacant particles") by $N_T R/(R+1)$. Here, N_T is a total number of both particles in the unit area of the plane and is roughly estimated as

$$N_T = \frac{1}{(\pi S_2^2)} . \tag{1}$$

Obviously, a group of vacant particles contact directly with each other, building a pore. Hereafter, we call this pore a vacant-particle pore (Figure 2c). A total number of vacant-particle pores per unit surface area (*i.e.*, pore density) is represented by N_P.

Assume that polymer particles and hypothetical vacant particles are placed randomly on a two-dimensional hexagonally close-packed lattice of the hypothetical plane to evaluate number of distinguishable arrangements of the mixtures of the polymer particles and the vacant particles on the lattice (Figures 2b and 2c). In this sense, the lattice coordination number is six. In the hypothetical planes of a gel membrane, a portion whose boundary is fully surrounded by polymer particles and which is concurrently occupied by the consecutively connected vacant particles yields a vacant-particle pore (Figure 2c). Here, we neglect the crevasse of the contacted polymer particles (Figure 2d), which will be discussed as inter-polymer-particle pore later.

The pore size can be approximately represented by the number x of vacant particles constituting a single vacant-particle pore. And a pore radius r distribution $N(r)$ for vacant-particle pores can be evaluated by translating a distribution of the number x of vacant particles constituting single pores on the hexagonal lattice sites. Consider the case when $N_T L$ vacant particles are divided into N_P cells. Here, L is volume fraction of polymer-lean phase given by the following equation,

$$L = \frac{R}{R+1} . \tag{2}$$

To ascertain the existence of N_P pores beforehand, one vacant particle is, in advance of counting, distributed to each cell. The number of ways, $W_{N_P}(N_T L - N_P)$ of partitioning the remaining $(N_T L - N_P)$ vacant particles into N_P cells is given by

$$W_{N_P}(N_T L - N_P) = \frac{\{(N_P - 1) + (N_T L - N_P)\}!}{(N_P - 1)!(N_T L - N_P)!} . \tag{3}$$

After ascertaining the existence of N_P vacant-particle pores by distributing one vacant particle to all N_P cells, a single pore, arbitrarily chosen, is fulfilled with $(x-1)$ vacant particles further to realize the pore with x vacant particles. Next, the number of ways, $W_{N_P-1}(N_T L - N_P - x + 1)$, of partitioning the remaining $(N_T L - N_P - x + 1)$ vacant particles into $(N_P - 1)$ pores (*i.e.*, all the pores except for the pore filled with x vacant particles and note that the single pore has already x vacant particles) is given by

$$W_{N_P-1}(N_T L - N_P - x + 1) = \frac{\{(N_P - 2) + (N_T L - N_P - x + 1)\}!}{(N_P - 2)!(N_T L - N_P - x + 1)!} . \tag{4}$$

Accordingly, when N_P pores are formed by partitioning $N_T L$ vacant particles, the desired probability $P(x)$ that x vacant particles are partitioned in a given pore is

$$P(x) = \frac{W_{N_P-1}(N_T L - N_P - x + 1)}{W_{N_P}(N_T L - N_P)} = \frac{(N_T L - x - 1)!(N_P - 1)!(N_T L - N_P)!}{(N_P - 2)!(N_T L - N_P - x + 1)!(N_T L - 1)!}$$

$$=\frac{(N_T L-N_P)(N_T L-N_P-1)\cdots(N_T L-N_P-x+2)(N_P-1)}{(N_T L-1)(N_T L-2)\cdots(N_T L-x)} . \quad (5)$$

Assuming that $N_P \gg 1$ and $N_T L - N_P \gg x$, eq 5 can be simplified into

$$P(x) \cong \frac{\left(1-\frac{N_P}{N_T L}\right)^x}{\left(\frac{N_T L}{N_P}-1\right)}$$

$$\text{for} \quad 1 \leq x < N_T L \quad \text{and} \quad N_P < N_T L . \quad (6)$$

On the other hand, for $N_P = N_T L$, x becomes unity and

$$P(x) = 1 . \quad (7)$$

It should be noted that $P(x)$ is normalized for the range of $x = 1$ to ∞,

$$\sum_{x=1}^{\infty} \frac{\left(1-\frac{N_P}{N_T L}\right)^x}{\left(\frac{N_T L}{N_P}-1\right)} = 1 . \quad (8)$$

Here, $N_T L$ vacant particles are consumed to build N_P pores and then the following equation of the boundary condition of vacant particles holds,

$$\sum_{x=1}^{N_T L} N_P x P(x) = N_T L . \quad (9)$$

By rewriting eq 9 average x can be defined as follows:

$$\bar{x} = \frac{N_T L}{N_P} \quad \text{for} \quad N_T L \gg 1 . \quad (10)$$

The radius of pore containing x vacant particles in wet gel membrane r_{Wet} is defined by the relation that area of a circular pore with radius r_{Wet} ($=\pi {r_{Wet}}^2$) is equal to the summation of area of the maximum cross section of x vacant particles ($=x\pi {S_2}^2$), that is

$$r_{Wet} = x^{1/2} S_2 . \quad (11)$$

When the radius of wet polymer particles S_2 decreases to S_2' during drying (Figure 3), the following equation holds.

$$\frac{4}{3}\pi {S_2'}^3 d_P' = \left(\frac{4}{3}\pi {S_2}^3\right) v_{P(2)} d_{PL} , \quad (12)$$

that is

$$S_2' = S_2 \left(\frac{v_{P(2)} d_{PL}}{d_P'}\right)^{1/3} , \quad (13)$$

where $v_{P(2)}$ is polymer volume fraction of the polymer rich-phase in equilibrium, and d_{PL} and d_P' are densities of the polymer itself and of the dried polymer particles, respectively. In other words, the volume of a polymer particle decreases to $(4\pi {S_2}^3/3) v_{P(2)} (d_{PL}/d_P')$ after drying.

Accordingly, the pore radius of dry membrane r is related to the pore radius r_{Wet} corresponding to S_2 of the wet gel membrane through the relation (Figure 3):

$$r = r_{Wet} + \left\{1 - \left(\frac{v_{P(2)} d_{PL}}{d_P'}\right)^{1/3}\right\} S_2 . \quad (14)$$

Combination of eq 11 with eq 14 gives

$$r = \left\{x^{1/2} + 1 - \left(\frac{v_{P(2)} d_{PL}}{d_P'}\right)^{1/3}\right\} S_2 . \quad (15)$$

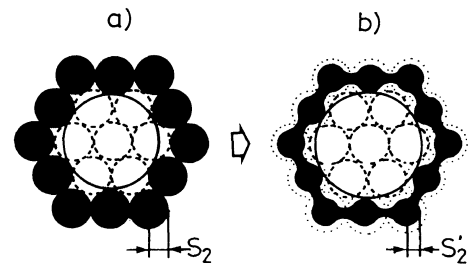

Figure 3. Change in a pore size during drying treatment under constant membrane width: a), A circular pore containing seven vacant particles (*i.e.*, $x=7$) in a wet gel membrane; filled circles, polymer particles; broken line circles, vacant particles; both kinds of particles have the same radius of S_2; b), An enlarged pore in a dry membrane; S_2', a radius of a dry polymer particle; $S_2' < S_2$ (see, eq 13).

At $x=1$, r given by eq 15 attains the minimum of radius of vacant-particle pore consisting of a single vacant particle, r_{min}:

$$r_{min}=\left\{2-\left(\frac{v_{P(2)}d_{PL}}{d_P'}\right)^{1/3}\right\}S_2 . \quad (16)$$

As the existing probability of the pore with the radius in the range from r to $(r+dr)$ is the same as that of the pore consisting of x to $(x+dx)$ vacant particles, the following relation holds:

$$\begin{pmatrix}\text{Probability density of}\\ \text{the pore with radius } r\end{pmatrix}\times dr = \begin{pmatrix}\text{Probability density of the pore}\\ \text{consisting of } x \text{ vacant particles}\end{pmatrix}\times dx$$

$$\frac{N_v(r)}{N_P}dr=P(x)dx \quad (17)$$

where $N_v(r)$ is the not-normalized pore radius distribution for vacant-particle pores which satisfies

$$\int_0^\infty N_v(r)dr=N_P . \quad (18)$$

Equation 17 can be rewritten to yield

$$N_v(r)=N_P P(x)\frac{dx}{dr} . \quad (19)$$

On the other hand, eq 15 can be rewritten as

$$x=\left[\frac{r}{S_2}-\left\{1-\left(\frac{v_{P(2)}d_{PL}}{d_P'}\right)^{1/3}\right\}\right]^2 \quad (20)$$

and differentiation of eq 20 by r gives

$$\frac{dx}{dr}=\frac{2}{S_2}\left[\frac{r}{S_2}-\left\{1-\left(\frac{v_{P(2)}d_{PL}}{d_P'}\right)^{1/3}\right\}\right] . \quad (21)$$

In deriving eq 21, we assume that $P(x)$ can be approximated by the continuous function and there exists one-to-one correspondence between x and r, in other words, all the pores in a plane have the same shape (that is, circular).

It should be noted that x is a function of r, S_2 and $v_{P(2)}$ at the constant d_{PL} and d_P' values and accordingly, $N_v(r)$ is a function of r, S_2, $v_{P(2)}$, N_P, and R in the forms:

$$x=x(r, S_2, v_{P(2)}) \quad (22)$$

and

$$N_v(r)=N_P P(x(r, S_2, v_{P(2)}), N_P, L(R))\times\frac{dx(r, S_2, v_{P(2)})}{dr} = N_v(r, S_2, v_{P(2)}, N_P, R) . \quad (23)$$

Combination of eq 6, 10, 19, 20, and 21 leads to

$$N_v(r)=\frac{2N_P}{S_2}\left(\frac{1}{\bar{x}-1}\right)\times\left(1-\frac{1}{\bar{x}}\right)^{\left[\frac{r}{S_2}-\left\{1-\left(\frac{v_{P(2)}d_{PL}}{d_P'}\right)^{1/3}\right\}\right]^2}\times\left[\frac{r}{S_2}-\left\{1-\left(\frac{v_{P(2)}d_{PL}}{d_P'}\right)^{1/3}\right\}\right] \quad \text{for } r\geq r_{min} \quad (24)$$

where

$$\bar{x}=\frac{R}{\pi S_2{}^2(R+1)N_P} . \quad (25)$$

Equation 25 is derived from eq 1, 2, and 10. From eq 24 it is clear that $N(r)$ for vacant-particle pores can be evaluated from R, S_2, and N_P data if $v_{P(2)}$, d_{PL}, and d_P' are given in advance.

Pore Density. $N_T L$ vacant particles are thus partitioned on N_T sites of the hexagonal lattice in the manner so as to build up N_P vacant-particle pores. However, a single vacant-particle pore should be an assembly of vacant particles, which can take various forms under the condition that at least any vacant particle contacts directly with another vacant particle or with other vacant particles directly. Consequently, this assembly can give pores with various pore shapes, which make further calculation extremely difficult. Then, for the sake of simplicity, we assume that the assembly of vacant particles (forming a single vacant-particle pore) has a strong tendency to form a

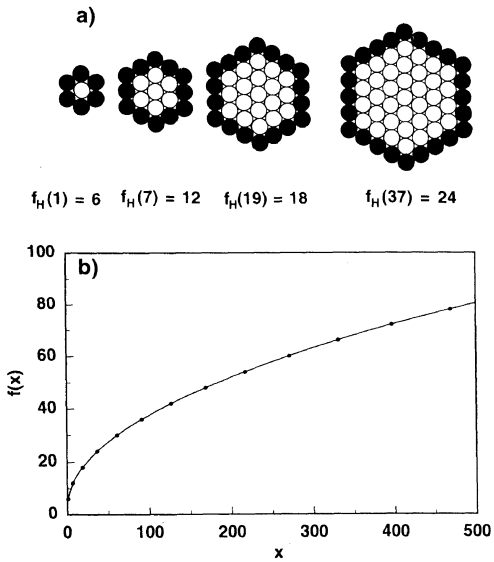

Figure 4. Approximation of a pore shape and number of polymer particles needed to surround an assembly of x vacant particles: a), Schematic representation of regular hexagonal pores consisting of x_H vacant particles which are fully surrounded by $f_H(x_H)$ polymer particles; $x_H=1$, $f_H(x_H)=6$; $x_H=7$, $f_H(x_H)=12$; $x_H=19$, $f_H(x_H)=18$; $x_H=37$, $f_H(x_H)=24$; b) Relationship between x and $f(x)$; points indicate x_H and $f_H(x_H)$ of regular hexagonal pores; full line, $f(x)=(12x-3)^{1/2}+3$.

circle and that on hexagonal lattice sites any assembly of vacant particles is regarded as hexagonal (Figure 4a).

When regular hexagonal vacant-particle pores consisting of x_H vacant particles are considered (*i.e.*, x_H can be 1, 7, 19, 37, $\cdots$, as is clear from Figure 4a), the minimum number of polymer particles needed to surround fully these regular hexagonal pores $f_H(x_H)$ is given by $\{(12x_H-3)^{1/2}+3\}$. If an assembly of vacant particles tends to form a circle, the length of its surrounding should be as short as possible, and in this case we can approximate the minimum number of polymer particles needed to surround fully an assembly of x vacant particles $f(x)$ by eq 26,

$$f(x)=\sqrt{12x-3}+3 \quad (x\geq 1)\,. \qquad (26)$$

In Figure 4b, full line is $f(x)$ and closed circles are $f_H(x_H)$.

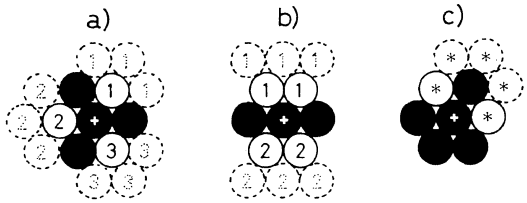

Figure 5. Some typical arrangements of polymer particles (filled circles) and vacant particles (unfilled circles) in the nearest neighbor of a given polymer particles (marked with +): m, number of vacant particles existing around the given polymer particle in the center of the nearest neighbor sites; n, number of different pores which the given polymer particle can participate to form when the six nearest neighbor sites around the given polymer particle are considered; vacant particles constituting a pore are drawn with bearing the pore number (no. 1—3); dotted circle, vacant particles existing possibly outside of the six nearest neighbor sites under consideration; a), $m=3$, $n=3$; b), $m=4$, $n=2$; c) Two not-directly connected vacant particles (unfilled circle with *) connect indirectly by contacting with other vacant particles outside of the six nearest neighbor sites in order to form a common pore (dotted circle with *).

Figure 5a shows that a given polymer particle marked with (+) mark on the lattice can contribute to the formation of at most three different pores when the six nearest neighbor sites of the given polymer particle are just considered. Here, these pores are numbered; 1, 2, and 3. In Figure 5b, a given polymer particle with (+) mark should be thought to participate in the formation of two different pores (no. 1 and 2).

When a single polymer particle is directly participated to the formation of n pores ($1\leq n\leq 3$), (1) the reciprocal n (*i.e.*, $1/n$) is defined as contribution fraction of the polymer particle to the formation of one vacant-particle pore, and (2) the number m of vacant particles existing around the particle (*i.e.*, the number of the nearest neighbor vacant particles) lies between 1 and 5 (*i.e.*, $1\leq m\leq 5$) and (3) the probability $P_n(m)$ that a given polymer particle is surrounded in part by m vacant particles, which belong to n different pores is shown in Table I. Here, we assume that probability of appearance of a vacant particle and a polymer particle in every seat on the lattice is the same

Table I. $P_n(m)$ values of hexagonal lattice

m	$P_n(m)$[a]			
	$n=0$	$n=1$	$n=2$	$n=3$
0	$(1\text{-}L)^6$	—	—	—
1	—	$6L(1-L)^5$	—	—
2	—	$6L^2(1-L)^4$	$9L^2(1-L)^4$	—
3	—	$6L^3(1-L)^3$	$12L^3(1-L)^3$	$2L^3(1-L)^3$
4	—	$6L^4(1-L)^2$	$9L^4(1-L)^2$	—
5	—	$6L^5(1-L)$	—	—

[a] —, no theoretical possibility of a given combination of m and n.

as L and (1-L), respectively. In other words, particles are distributed on the hexagonal lattice randomly. When vacant particles are assumed to gather circularly, we can neglect the possibility that two not-directly connected vacant particles, which are the nearest neighbor of a given polymer particle, belong to a common pore (Figure 5c), and $P_1(4)\approx 0$ and $P_1(5)\approx 0$ are expected.

Reciprocal n, $1/n$ can be averaged over all possible arrangements of the vacant particles and polymer particles around a distinguishable polymer particle:

$$\left(\overline{\frac{1}{n}}\right)=\frac{\sum_{n=1}^{3}\left\{\sum_{m=1}^{5}\frac{1}{n}P_n(m)\right\}}{\sum_{n=1}^{3}\left\{\sum_{m=1}^{5}P_n(m)\right\}}. \qquad (27)$$

Then, it is clear that $\overline{(1/n)}$ is determined by the volume fraction of polymer-lean phase L, accordingly by the two-phase volume ratio R.

In this manner, in order to form N_P vacant-particle pores, $N_T L$ vacant particles are partitioned into N_P hexagonal assemblies. The number of the assemblies, each consisting of x vacant particles, is $N_P P(x)$ and the number of polymer particles consumed in order to surround fully an assembly with x vacant particles, $f(x)$, is given by eq 26.

The total number of the polymer particles directly surrounding N_P independent pores should be the total number of the polymer particles which contribute to form vacant-particle pores;

$$\sum_{x=1}^{N_T L}\left\{\begin{pmatrix}\text{Number of vacant-}\\ \text{particle pores}\\ \text{consisting of } x\\ \text{vacant particles}\end{pmatrix}\times\begin{pmatrix}\text{Number of polymer particles}\\ \text{surrounding the vacant-}\\ \text{particle pore consisting}\\ \text{of } x \text{ vacant particles}\end{pmatrix}\times\begin{pmatrix}\text{Average contribution fraction of one}\\ \text{polymer particle to the formation}\\ \text{of one vacant-particle pore}\end{pmatrix}\right\}$$
$$=\begin{pmatrix}\text{Total number of}\\ \text{polymer particles}\end{pmatrix}\times\begin{pmatrix}\text{Probability that a given}\\ \text{polymer particle contributes}\\ \text{to form vacant-particle pores}\end{pmatrix},$$

that is

$$\sum_{x=1}^{N_T L}N_P P(x)f(x)\left(\overline{\frac{1}{n}}\right)=N_T(1-L)\left[1-\frac{P_0(0)}{\sum_{n=0}^{3}\left\{\sum_{m=0}^{5}P_n(m)\right\}}\right]$$
$$=N_T(1-L)\left[\frac{\sum_{n=1}^{3}\left\{\sum_{m=1}^{5}P_n(m)\right\}}{\sum_{n=0}^{3}\left\{\sum_{m=0}^{5}P_n(m)\right\}}\right], \qquad (28)$$

which is the boundary condition of polymer particles.

Equation 28 can be rewritten as follows:

$$N_P=\frac{N_T(1-L)\left[\frac{\sum_{n=1}^{3}\left\{\sum_{m=1}^{5}P_n(m)\right\}}{\sum_{n=0}^{3}\left\{\sum_{m=0}^{5}P_n(m)\right\}}\right]}{\left(\overline{\frac{1}{n}}\right)\sum_{x=1}^{N_T L}f(x)P(x)}$$

$$N_T(1-L)\frac{\left[\sum_{n=1}^{3}\left\{\sum_{m=1}^{5}P_n(m)\right\}\Big/\sum_{n=0}^{3}\left\{\sum_{m=0}^{5}P_n(m)\right\}\right]}{\left(\frac{1}{n}\right)\overline{f(x)}} \quad (\text{for } N_TL \gg 1)$$

$$= \frac{\left(\begin{array}{c}\text{Total number of polymer}\\ \text{particles which contribute to}\\ \text{form vacant-particle pores}\end{array}\right)}{\left(\begin{array}{c}\text{Average number of polymer}\\ \text{particles which contribute to}\\ \text{form one vacont-particle pore}\end{array}\right)} \quad (29)$$

When we employ $P_n(m)$ given by Table I, in other words, polymer particles and vacant particles are placed randomly on the lattice, eq 28 always holds its validity. Here, we define N_P value, which satisfies eq 28, as $N_{P(v)}$. N_P decreases when vacant particle has a tendency to be partitioned in the nearest neighbor of another vacant particle. $N_{P(v)}$ should be taken as N_P theoretically expected for a given combination of R and S_2 under the random distribution of particles.

Accordingly, if R and S_2 are given and values of N_T, L and $\overline{(1/n)}$ are calculable, we can obtain $N_{P(v)}$ numerically. Route of calculation of $N_{P(v)}$ for vacant-particle pores is illustrated in Figure 6. Note that $N_{P(v)} < N_TL$ (*i.e.*, $\bar{x} > 1$) should always hold. For $N_{P(v)} = N_TL$, eq 7 is used instead of eq 6.

Inter-Polymer-Particle Pore

Even if the polymer particles occupy all the sites of the hexagonal close-packed lattice (*i.e.*, $R=0$), there are numerous small crevasses between the polymer particles and such crevasses act as pores, as in the case of reverse osmosis membranes, and are hereafter referred to as inter-polymer-particle pores (Figure 2d) in order to distinguish them from the vacant-particle pores and the crevasse in wet gel membrane becomes large during drying when the dimension of the membrane is kept constant.

Consider a polymer particle with m nearest neighbor vacant particles, belonging to n different pores and having $n_{(i)}$ inter-polymer-particle pores. When $m=0$ (and accordingly, $n=0$), $n_{(i)}=6$ is obtained. In this manner, we can calculate $n_{(i)}$ value for a given combination of m and n, as shown in Figure 7. Cases such as $m=0$ and $n=1$ are not theoretically realized and shown as blanks with a slash mark in Figure 7. In a case of $m=3$ and $n=3$, there is

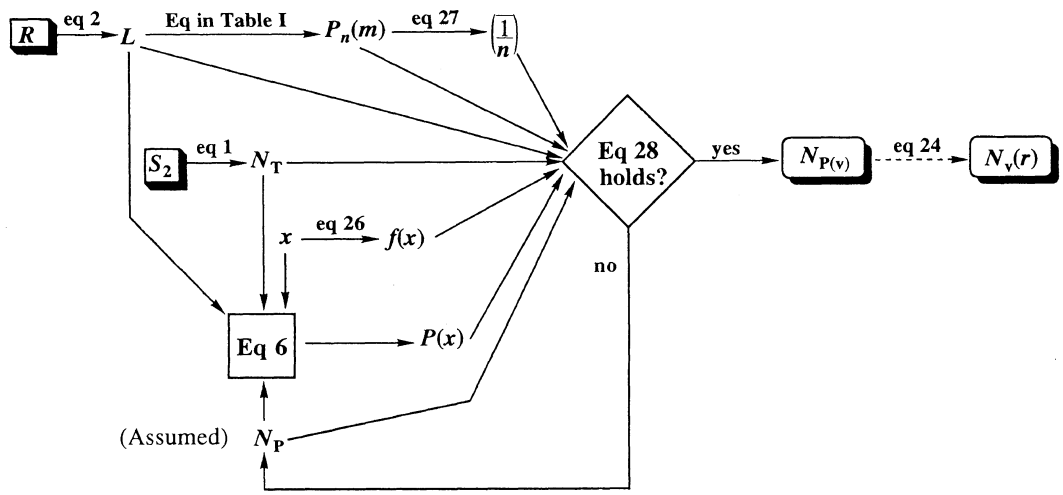

Figure 6. Route of calculation of $N_{P(v)}$ for vacant-particle pores from R and S_2.

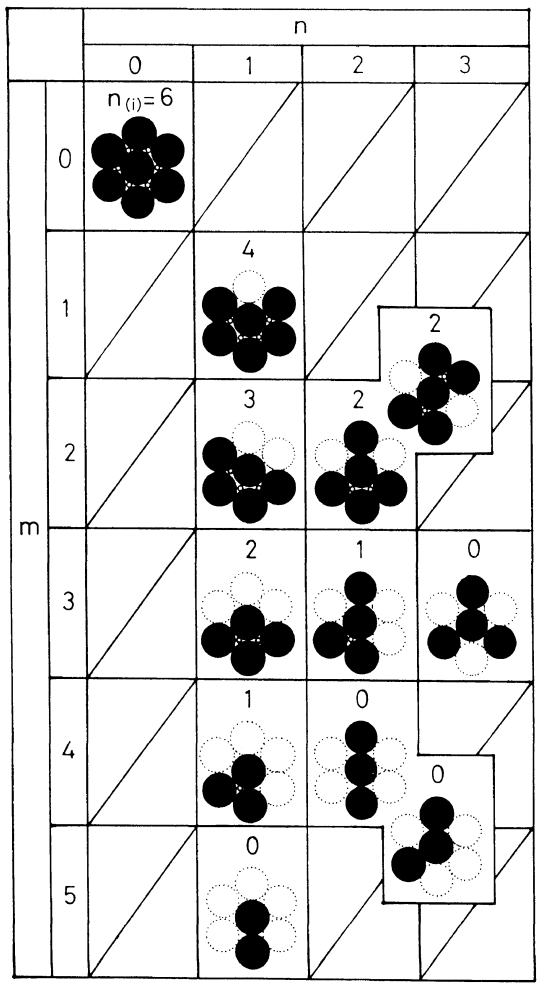

Figure 7. Theoretically possible arrangements of inter-polymer-particle pores existing around a given polymer particle: Six nearest neighbor sites around a given polymer particle are just considered; $n_{(i)}$, number of the inter-polymer-particle pores; m, number of vacant particles existing around the given polymer particle in the center; n, number of different pores which the given polymer particle can participate to form; filled circle, polymer particle; dotted unfilled circle, vacant particle; small unfilled circle, inter-polymer-particle pore.

no probability of finding inter-polymer particle pores (*i.e.*, $n_{(i)}=0$).

Then, the average number of inter-polymer-particle pores directly contacted with a given single polymer particle, $\overline{n_{(i)}}$ is given by

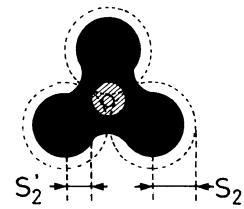

Figure 8. Change in pore size of an inter-polymer particle pore after drying: Broken line circle, wet polymer particle; full line circle in hatched area, wet inter-polymer-particle pore; S_2, radius of a wet polymer particle; S_2', radius of a dry polymer particle; hatched area, inter-polymer particle pore after drying; blacked area, dry polymer particle.

$$\overline{n_{(i)}}=\frac{\sum_{n=0}^{3}\left\{\sum_{m=0}^{5} n_{(i)}P_n(m)\right\}}{\sum_{n=0}^{3}\left\{\sum_{m=0}^{5} P_n(m)\right\}}. \tag{30}$$

As one inter-polymer-particle pore contacts three polymer particles, a number of inter-polymer-particle pores in unit area of a membrane $N_{P(i)}$ is

$$N_{P(i)}=\frac{N_T(1-L)\overline{n_{(i)}}}{3}. \tag{31}$$

An inter-polymer-particle pore is formed by mutual contact of three polymer particles and the radius of the inter-polymer-particle pore, $r_{(i)Wet}$ of a wet gel membrane, which is noticed by the radius of an inscribed circle, is related to S_2 through the relation,

$$r_{(i)Wet}=\left(\frac{2}{\sqrt{3}}-1\right)S_2. \tag{32}$$

After drying S_2 changes to S_2' (eq 13), keeping its center at the same position, as shown in Figure 8 and the radius of the inter-polymer-particle pore of dry membrane $r_{(i)}$ is readily obtained by adding the difference between S_2 and S_2' in eq 13 to $r_{(i)Wet}$ in eq 32:

$$r_{(i)}=r_{(i)Wet}+(S_2-S_2')$$
$$=\left(\frac{2}{\sqrt{3}}-1\right)S_2+\left\{1-\left(\frac{v_{P(2)}d_{PL}}{d_P'}\right)^{1/3}\right\}S_2$$

$$=\left\{\frac{2}{\sqrt{3}}-\left(\frac{v_{p(2)}d_{PL}}{d_P'}\right)^{1/3}\right\}S_2 \,. \qquad (33)$$

The pore size distribution $N(r)$ for inter-polymer-particle pores, denoted by $N_i(r)$ can be given as:

$$N_i(r)=N_{P(i)}\delta(r-r_{(i)}) \qquad (34)$$

where $\delta(r)$ is the δ-function which satisfies

$$\int_{-\infty}^{\infty}\delta(r)\mathrm{d}r=1 \,. \qquad (35)$$

Schema of calculating $N_{P(i)}$ and $N_i(r)$ is shown in Figure 9. Note again that eq 24 and 34 are derived assuming that the super-particle structure (morphology) of coagulated polymer particles does not change through collapse during the phase separation (step f of Figure 1), the coagulation (step g) and drying (step j). At a latter step, radius of the polymer particle changes only by a factor of $(v_{p(2)}d_{PL}/d_P')$.

Porosity of Membranes

Gel Membranes. Suppose that a polymer solution is cast on a plate to give a thin solution film with a thickness of L_0 (Figure 10a): In wet method, the cast solution is dipped in a coagulating solution consisting of non-solvent(s). In dry method, the cast solution is settled in an atmosphere of nonsolvent(s). Phase separation occurs at the surface of the cast solution and it proceeds from the surface to the inner part of solution (Figures 10g and

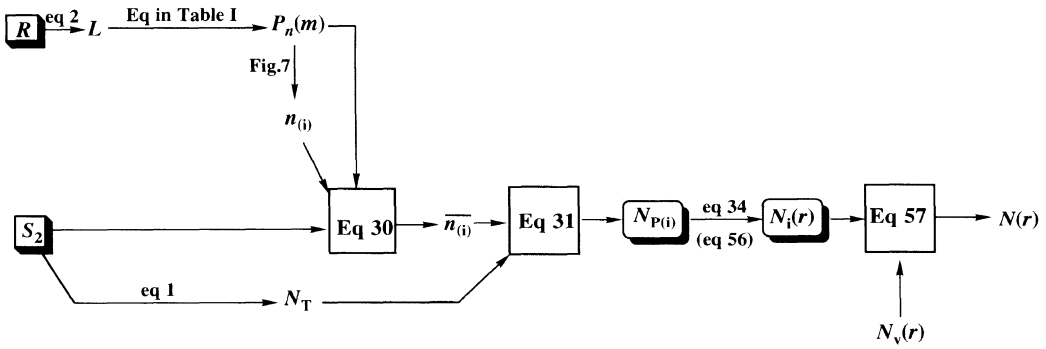

Figure 9. Route of calculation of $N_{P(i)}$ and $N_i(r)$ for inter-polymer-particle pores from R and S_2.

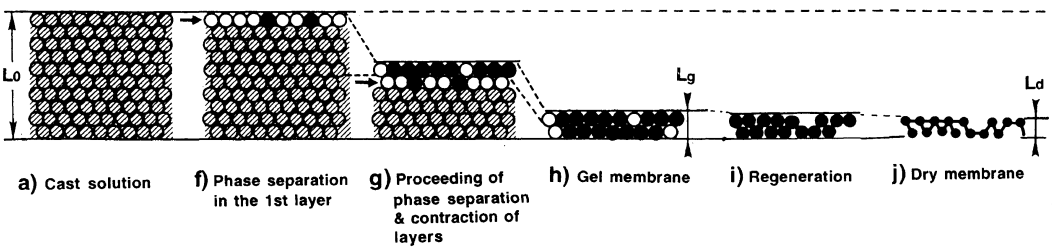

Figure 10. Schematic representation of changes of membrane thickness during membrane formation process: a), Casting of polymer solution; f), Starting of the phase separation; g), Proceeding of phase separation and contraction of thin layers; h), Gel membrane (end of the over-all phase separation); i), Regeneration; j), Dry membrane; unfilled circle, vacant particle; filled circle, polymer particle; hatched area, homogeneous polymer solution not yet phase-separated; unfilled circle in the hatched area, position of particles to be created by phase separation; L_0, thickness of cast solution; L_g, thickness of gel membrane; L_d, thickness of dry membrane; arrows indicate a layer where the phase separation has just occurred and the layer-contraction has not occurred yet; steps a and f—j correspond to those of a and f—j in Figure 1, respectively.

10h). We define the volume fraction of a polymer-lean phase in a hypothetical layer at the moment of phase separation as $Pr(\mathrm{PS})$, which is given by the relation

$$Pr(\mathrm{PS})=\frac{R}{R+1}. \tag{36}$$

During the progress of phase separation, the thickness of the cast solution decreases and a coagulated gel membrane with thickness L_g is formed (Figure 10h). The volume fraction of vacant particles in the gel membrane $Pr(\mathrm{GEL})$ is governed by the degree of collapse of thin layers.

In a case where two hypothetical layers having the same $Pr(\mathrm{PS})$ collapse into a "single layer", it is required that a vacant particle in the upper layer is just superposed with another vacant particle in the lower layer in order to find a vacant particle in the "single layer". The probability of occurrence of the above phenomenon (*i.e.*, the porosity) is $\{Pr(\mathrm{PS})\}^2$. Accordingly, $Pr(\mathrm{GEL})$ is equal to the porosity of a "single layer" formed by the collapse of k hypothetical layers is given by

$$Pr(\mathrm{GEL})=\{Pr(\mathrm{PS})\}^k=\left(\frac{R}{R+1}\right)^k. \tag{37}$$

Here, the following relation holds approximately:

$$k\cong\frac{L_0}{L_g}. \tag{38}$$

The porosity of gel membranes consisting of collapsed hypothetical layers, $Pr(\mathrm{GEL})$ is equivalent with apparent volume fraction of polymer-lean phase L_A.

Next, we define apparent phase volume ratio R_A by the relation

$$R_A=\frac{\left(\frac{R}{R+1}\right)^k}{1-\left(\frac{R}{R+1}\right)^k}. \tag{39}$$

For the gel membranes formed after collapse of hypothetical layers, R in eq 25 should be substituted with R_A in calculation of $N(r)$.

L_A ($=Pr(\mathrm{GEL})$) is defined by

$$L_A=\frac{R_A}{R_A+1} \tag{40}$$

and it should be substituted with L in calculation of eq 3—6, eq 8—10, eq 27—31, and equations in Table I.

Dry Membranes. After gel membranes with thickness L_g are formed, the membrane is treated with acid for generation of cellulose (if necessary) and washed and dried.

Considering an increase in volume of both vacant-particle pores and inter-polymers-particle pores due to de-solvation of polymer particles in drying step, the porosity of dry membrane $Pr(\mathrm{d})$ (as denoted by $Pr(\mathrm{d}_1)$) is given by eq 41,

$$\begin{aligned}Pr(\mathrm{d}_1)&=\left\{1-\left(\frac{S_2'}{S_2}\right)^3\right\}(1-L_A)+L_A\\&=\left(1-\frac{v_{p(2)}d_{PL}}{d_P'}\right)(1-L_A)+L_A.\end{aligned} \tag{41}$$

S_2' is the radius of dry polymer particle (see, eq 13). In deriving eq 41, it is assumed that pore density N_P does not change during drying step, and $Pr(\mathrm{d}_1)$ represents the summation of porosity of vacant-particle pores and that of inter-polymer-particle pores.

EXPERIMENTAL

Preparation of Cellulose Membranes

Cellulose cuprammonium solution with the cellulose concentration (weight fraction) $w_{Cell}=0.04$ to 0.09 was prepared by diluting with ammonium-water solution (the weight fraction of ammonia $w_{NH_3}=0.28$) an original cellulose cuprammonium solution, whose compositions were $w_{Cell}=0.10$, the weight fraction of copper $w_{Cu}=0.0395$, $w_{NH_3}=0.0703$, and the weight fraction of water $w_{H_2O}=0.7902$.

Cellulose cuprammonium solutions with w_{Cell}

of 0.04 to 0.10 were cast on flat glass plates, respectively. The cast solutions, having 500 μm thickness ($=L_0$), cast on the glass plates, were immersed in a coagulating solution containing acetone, ammonia and water (the weight fraction of acetone $w_{\text{Acetone}}:w_{\text{NH}_3}:w_{\text{H}_2\text{O}}=0.30:0.0056:0.6944$) at 298.15 K. After coagulation, the gel membranes were peeled off from the glass plates and treated with sulfuric acid-water solution (the weight fraction of sulfuric acid = 0.02) at 293.15 K, and then washed with water. The wet membranes were immersed in acetone and then dried at 298.15 K under fixed length without dimensional change. Thickness of dry membrane L_{d} was measured by using an upright dial gauge (manufactured by Ozaki Seisakusho Co., Japan).

Membranes thus prepared were embedded in blocked acrylic resin (a mixture of *n*-butyl acrylate and methyl methacrylate) and sliced using Ultrotome® type 8800 (manufactured by LKB., Sweden) in parallel to the membrane surface to give thin sections of 1 μm thickness. The acrylic resin for embedding was removed by dissolving with chloroform. The sections obtained from their top surfaces were employed in scanning electron microscopic observation.

Measurements

Porosities of Membranes. The porosity of dry membrane was directly evaluated from apparent density d_{A} of the membrane and density of polymer constructing the membrane d_{PL} through use of eq 42a. The porosity, determined by this method (apparent density method) was denoted as $Pr(\text{d}_3)$,

$$Pr(\text{d}_3)=1-\frac{d_{\text{A}}}{d_{\text{PL}}} \tag{42a}$$

where $d_{\text{A}}=w_{\text{m}}/v_{\text{m}}$ (w_{m}, v_{m} are weight and volume of absolutely dry membrane, respectively). All pores such as through pores, semi-open pores, and independent pores[3] existing in the membrane, and also cracks in polymer particles contribute to $Pr(\text{d}_3)$.

An effect of the cracks in polymer particles on $Pr(\text{d}_3)$ can be omitted if d_{P}' was used in eq 42a instead of d_{PL}. We can estimate a real porosity of dry membrane $Pr(\text{d}_3)'$ by the relation:

$$Pr(\text{d}_3)'=1-\frac{d_{\text{A}}}{d_{\text{P}}'}. \tag{42b}$$

Another kind of porosity of dry membrane $Pr(\text{d}_4)$ was determined from electron micrographs by eq 43,[8]

$$Pr(\text{d}_4)(\equiv Pr(\text{EM}))=\frac{\sum_i L_{\text{C},i}}{\sum_i L_i} \tag{43}$$

where L_i is the length of the i-th test lines drawn on a photograph of membrane surface and $L_{\text{C},i}$ is the cut-off length, by pores, of the i-th test line. $Pr(\text{d}_4)$ neglects the contribution of pores smaller than the resolution power of the scanning electron microscope employed and is suitable for the determination of the porosity of thin membrane or membrane whose whole pore characteristics can be well represented by those at the surface.

Density of dried polymer particles. Assuming that $Pr(\text{d}_3)'$ is equal to $Pr(\text{d}_4)$ and combining of eq 42a, 42b, and 43, the density of dried polymer particles d_{P}' is given by eq 44,

$$d_{\text{P}}'=\frac{\{1-Pr(\text{d}_3)\}d_{\text{PL}}}{\{1-Pr(\text{d}_4)\}}. \tag{44}$$

Electron micrographic method for determination of S_2' and $N(r)$. Electron micrographs (EM) on the surface of membranes were taken using a field emission scanning electron microscope (FE-SEM S-800, manufactured by Hitachi, Ltd., Tokyo, Japan) and S_2' was determined directly from the EM by averaging radii of polymer particles. The pore radius distribution $N(r)$ was evaluated from the EM by a stereological method.[5]

Phase Equilibria. Cellulose cuprammonium solutions with $w_{\text{Cell}}=0.05$ and 0.08 were

prepared by adding ammonia-water solution ($w_{NH_3}=0.28$) to an original cellulose cuprammonium solution ($w_{Cell}=0.10$, $w_{Cu}=0.0395$, $w_{NH_3}=0.0703$, $w_{H_2O}=0.7902$). A given amount of the solution was poured into a closed glass vessel, to which a predetermined amount of acetone-water solution ($w_{Acetone}=0.30$) was added, agitated sufficiently, stocked for a whole day at 298.15 K, then the two phase volume ratio R was measured.

The largest R value, R_{max} was obtained when the experimentally permissible minimum amount of acetone-water solution, which brings about two-phase separation, was added to the cuprammonium solution, and we regarded that R_{max} corresponded to the casting condition of an actual membrane.

RESULTS AND DISCUSSION

Theoretical Predictions of the Correlation between the Casting Conditions and the Pore Characteristics of Membranes

Figure 11 shows the effect of the pore density N_P on pore size distribution $N(r)$, as estimated by eq 24, in two cases: $R=0.25$ and $S_2=250$ nm (Figure 11a), and $R=1.0$ and $S_2=250$ nm (Figure 11b). Other conditions are kept constant; $v_{p(2)}=0.3$, $d_{PL}=1.5\times10^3\,kg\,m^{-3}$, and $d_P'=0.9\times10^3\,kg\,m^{-3}$. With an increase in N_P, $N_v(r)$ becomes sharper and its peak shifts to smaller r region. Pore radius r which gives the peak of $N_v(r)$, r_{peak}, and $N_v(r_{peak})$ are given by the following equations, respectively:

$$r_{peak}=\left[\left\{1-\left(\frac{v_{p(2)}d_{PL}}{d_P'}\right)^{1/3}\right\}+\frac{1}{\sqrt{2\ln\dfrac{\bar{x}}{\bar{x}-1}}}\right]S_2 \tag{45}$$

and

$$N_v(r_{peak})=\frac{2N_P}{S_2}\times\frac{\left(1-\dfrac{1}{\bar{x}}\right)^{\left(2\ln\frac{\bar{x}}{\bar{x}-1}\right)^{-1}}}{(\bar{x}-1)\sqrt{2\ln\dfrac{\bar{x}}{\bar{x}-1}}}. \tag{46}$$

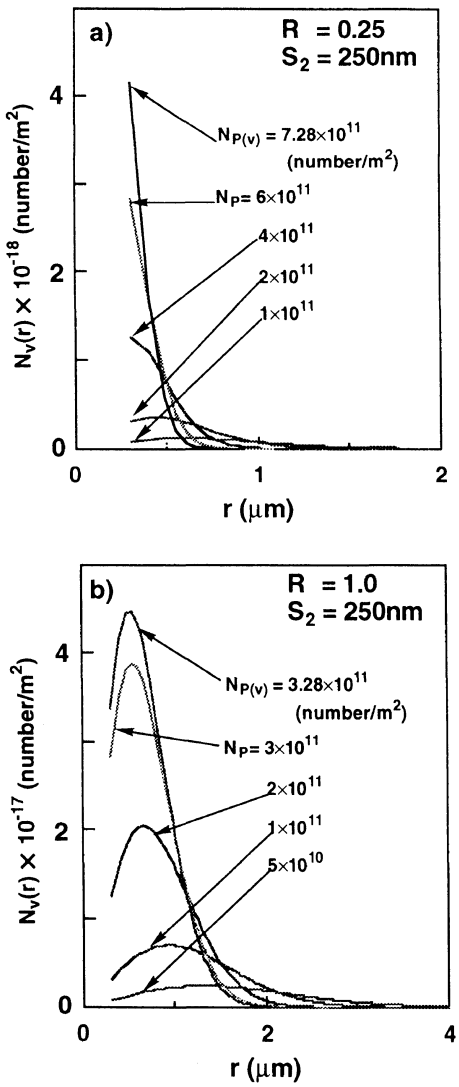

Figure 11. Effect of the pore density N_P on the pore size distribution $N_v(r)$ (eq 24): Radius of a polymer particle S_2, 250 nm; $N_{P(v)}$, calculated along a route in Figure 6; $v_{p(2)}$, 0.3; d_{PL}, $1.5\times10^3\,kg\,m^{-3}$; d_P', $0.9\times10^3\,kg\,m^{-3}$; a), Phase volume ratio R, 0.25; b), R, 1.0.

The criteria that $N(r)$ has a peak at $r>r_{min}$ is $r_{peak}>r_{min}$. This expression can be rewritten using eq 45 for r_{peak} and eq 16 for r_{min} in the form,

$$\bar{x}>\frac{1}{1-e^{-1/2}}\ (\approx2.54)\,. \tag{47}$$

Equation 47 can be again rewritten as a

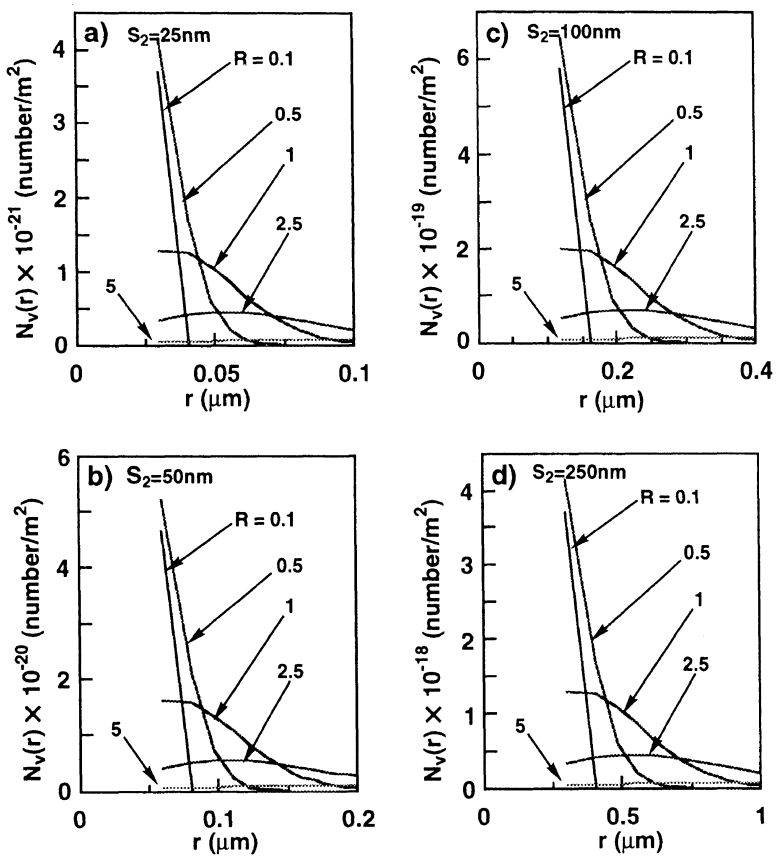

Figure 12. Effect of the two-phase volume ratio R on the pore size distribution $N_v(r)$ (eq 24): Values of S_2, R, and $N_{P(v)}$ used in calculations and those of $\bar{x}$, R'_{peak}, and r_{peak} obtained are listed in Table II; $v_{p(2)}$, 0.3; d_{PL}, 1.5×10^3 kg m^{-3}; d_P', 0.9×10^3 kg m^{-3}.

function of S_2 and R in the form,

$$N_P < \frac{R(1-e^{-1/2})}{\pi S_2{}^2(R+1)} (\equiv N'_{P,peak}) . \quad (47a)$$

The peak disappears at $N_P \geq 4\times10^{11}$ (number m^{-2}) in Figure 11a. As $N_{P(v)}$ ($=3.28\times10^{11}$ (number m^{-2})) is smaller than $N'_{P,peak}$ ($\approx 1\times10^{12}$ (number m^{-2})) in Figure 11b, $N_v(r)$ always has a peak.

Equation 47 can also be rewritten as a function of S_2 and N_P in the form,

$$R > \frac{\pi S_2{}^2 N_P}{1-e^{-1/2}-\pi S_2{}^2 N_P} (\equiv R'_{peak}) . \quad (47b)$$

As far as eq 47b holds its validity, $N_v(r)$ has a peak.

Figure 12 shows the effect of the two-phase volume ratio R on the pore size distribution $N_v(r)$ when $S_2=25$, 50, 100, and 250 nm and N_P is taken as $N_{P(v)}$ (*i.e.*, random distribution of particles is attained). Other conditions are kept constant; $v_{p(2)}=0.3$, $d_{PL}=1.5\times10^3$ kg m^{-3}, and $d_P'=0.9\times10^3$ kg m^{-3}. With an increase in R, the breadth of pore size distribution curve increases significantly with a shift of its peak to the larger r side.

When polymer particles are placed randomly on the lattice (*i.e.*, $N_P=N_{P(v)}$), the effect of the radius of the polymer particles S_2 on the pore size distribution $N_v(r)$ can not be clarified by simply taking both R and N_P constant, because $N_{P(v)}$ changes in proportion to $1/(S_2)^2$ even at

constant R. Combining eq 1, 2, and 29, we obtain eq 48. The equation indicates that $S_2{}^2N_{P(v)}$ is constant at constant R (*i.e.*, constant L). Average x, $\bar{x}$ (eq 10) also becomes constant for given R. $N_{P(v)}$, which was numerically determined by using eq 28, and $\bar{x}$, R'_{peak} and r_{peak} for various S_2 are listed in Table II.

Table II. $N_{P(v)}$, $\bar{x}$, R'_{peak}, and r_{peak} for various S_2 and R

S_2 / nm	R	$N_{P(v)}$ (number/ m^2)	$\bar{x}$ (number/ pore)	R'_{peak}	r_{peak}[a] / nm
10	0.1	2.05×10^{14}	1.41	0.196	—
	0.25	2.95×10^{14}	2.16	0.308	—
	0.5	2.78×10^{14}	3.82	0.285	14.9
	1	1.73×10^{14}	9.21	0.160	22.9
	2.5	4.64×10^{13}	49.0	0.038	51.3
	5	1.29×10^{13}	206	0.010	103.5
25	0.1	3.29×10^{13}	1.41	0.196	—
	0.25	4.72×10^{13}	2.16	0.308	—
	0.5	4.45×10^{13}	3.82	0.285	37.2
	1	2.77×10^{13}	9.21	0.160	57.3
	2.5	7.43×10^{12}	49.0	0.038	128.3
	5	2.06×10^{12}	206	0.010	258.8
50	0.1	8.22×10^{12}	1.41	0.196	—
	0.25	1.18×10^{13}	2.16	0.308	—
	0.5	1.11×10^{13}	3.82	0.285	74.5
	1	6.29×10^{12}	9.21	0.160	114.6
	2.5	1.86×10^{12}	49.0	0.038	256.6
	5	5.14×10^{11}	206	0.010	517.6
100	0.1	2.05×10^{12}	1.41	0.196	—
	0.25	2.95×10^{12}	2.16	0.308	—
	0.5	2.78×10^{12}	3.82	0.285	148.9
	1	1.73×10^{12}	9.21	0.160	229.2
	2.5	4.64×10^{11}	49.0	0.038	513.2
	5	1.29×10^{11}	206	0.010	1035.1
250	0.1	3.29×10^{11}	1.41	0.196	—
	0.25	4.72×10^{11}	2.16	0.308	—
	0.5	4.45×10^{11}	3.82	0.285	372.3
	1	2.77×10^{11}	9.21	0.160	572.9
	2.5	7.43×10^{10}	49.0	0.038	1282.9
	5	2.06×10^{10}	206	0.010	2587.8
500	0.1	8.22×10^{10}	1.41	0.196	—
	0.25	1.18×10^{11}	2.16	0.308	—
	0.5	1.11×10^{11}	3.82	0.285	744.6
	1	6.92×10^{10}	9.21	0.160	1145.9
	2.5	1.86×10^{10}	49.0	0.038	2565.8
	5	5.14×10^{9}	206	0.010	5175.7

[a] $v_{P(2)}=0.3$; $d_{PL}=1.5\times10^3$ kg m^{-3}; $d_P'=0.9\times10^3$ kg m^{-3}.

$$S_2{}^2N_{P(v)} = \frac{\sum_{n=1}^{3}\left\{\sum_{m=1}^{5}P_n(m)\right\}}{\pi(R+1)\left(\overline{\frac{1}{n}}\right)\overline{f(x)}\left[\sum_{n=0}^{3}\left\{\sum_{m=0}^{5}P_n(m)\right\}\right]} = \text{constant}. \quad (48)$$

From Figure 12, we can evaluate the effect of S_2 on $N_v(r)$ under the condition of constant R; $N_v(r)$ becomes narrower and its peak becomes higher to a large extent with decrease in S_2.

When N_P in eq 24 is taken as $N_{P(v)}$, $N_v(r)$ for given R can be represented by a master curve in the form,

$$N^*(r^*)=\left(\frac{1}{\bar{x}-1}\right)\times\left(1-\frac{1}{\bar{x}}\right)^{\left[r^*-\left\{1-\left(\frac{v_{P(2)}d_{PL}}{d_P'}\right)^{1/3}\right\}\right]^2}\times\left[r^*-\left\{1-\left(\frac{v_{P(2)}d_{PL}}{d_P'}\right)^{1/3}\right\}\right] \quad \text{for} \quad r^*\geq 2-\left(\frac{v_{P(2)}d_{PL}}{d_P'}\right)^{1/3} \quad (49)$$

where $r^*=r/S_2$ and $N^*(r^*)=N_v(r)S_2/2N_{P(v)}$.

Figure 13 shows the plots of $N^*(r^*)$ *versus* r^* for given R. The plot is a "master curve." With an increase in R, the curve becomes broader and the peak height decreases and the peak location shifts to the lager r/S_2 side. In Table II, R'_{peak} (eq 47b) and r_{peak} (eq 45) are also listed. When $R>R'_{peak}$, $N_v(r)$ has a peak for $r>r_{min}$. $N_v(r)$s for R above 0.5 in Figure 13 have peaks at $r=r_{peak}$.

Both our theory and the computer experiments on the thermodynamics of phase separation indicate that the larger phase volume ratio R will be realized when a polymer with lower weight-average degree of polym-

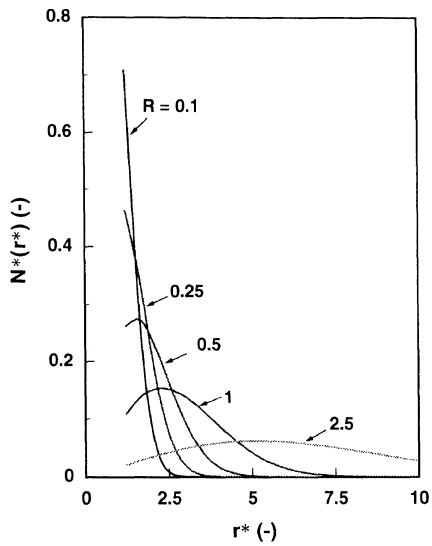

Figure 13. Effect of the two-phase volume ratio R on the relation between $N^*(r^*)$ and r^*: Value of R is shown in the figure; $v_{p(2)}$, 0.3; d_{PL}, 1.5×10^3 kg m^{-3}; d_P', 0.9×10^3 kg m^{-3}.

erization X_w and broader molecular distribution X_w/X_n (X_n, the number-average degree of polymerization) is dissolved in a single solvent having larger p_1 (1st order concentration-dependent parameter of thermodynamic interaction parameter χ between solvent and polymer)[9-15] or in a binary solvent mixture with smaller χ_{12}, larger χ_{13}, smaller χ_{23} ($\chi_{12}{}^0$, $\chi_{13}{}^0$, $\chi_{23}{}^0$; thermodynamics interaction parameter between solvent and nonsolvent, solvent and polymer, and nonsolvent and polymer, respectively)[16-18] to give a dilute solution, which is phase-separated under the condition of a larger relative amount of polymer precipitated, ρ_p.

Porosity and Phase Volume Ratio

If contribution of inter-polymer-particle pores can be neglected, $Pr(d_1)$ (eq 41) should be compared with the porosity of dry membrane $Pr(d)$ (in this case $Pr(d_2)$) estimated through use of eq 50,[4]

$$Pr(d_2)=\pi N_P \bar{r}^2 \tag{50}$$

where average pore radius $\bar{r}$ is defined using eq 10 and 15 by

$$\bar{r}=\left\{\bar{x}^{1/2}+1-\left(\frac{v_{P(2)}d_{PL}}{d_P'}\right)^{1/3}\right\}S_2 . \tag{51}$$

When volumetric increase due to inter-polymer-particle pores during drying step are considered, $Pr(d_2)'$ should be used as the porosity of dry membrane:

$$Pr(d_2)'=\pi\{N_{P(v)}\bar{r}^2+N_{P(i)}r_{(i)}{}^2\} . \tag{52}$$

Table III lists the various kinds of the porosity defined above. Combining eq 40 and 41, we obtain

$$v_{P(2)}=\frac{\{1-Pr(d_1)\}(R_A+1)d_P'}{d_{PL}} . \tag{53}$$

Giving R_A an appropriate value which satisfies the relation of $Pr(d_1)=Pr(d_2)'$ under the assumption of $Pr(d_1)=Pr(d_4)$, we can determine $v_{p(2)}$ and R_A by eq 53.

Collapse of Gel Membrane and its Porosity

Cellulose cuprammonium solution cast on a glass plate (step a in Figure 10) contracts to give a gel membrane with a thickness of *ca.* 1/5 of the cast solution ($L_g\approx L_0/5$) and the thickness of dry membrane L_d becomes *ca.* 1/10 of L_0 ($L_d\approx L_0/10$). Equation 39 reduces to eq 54 when k is assumed to be k' given by eq 55,

$$R=\frac{\left(\frac{R_A}{R_A+1}\right)^{1/k'}}{1-\left(\frac{R_A}{R_A+1}\right)^{1/k'}}, \tag{54}$$

where

$$k'=\frac{L_0}{L_d} . \tag{55}$$

k' values for regenerated cellulose membranes prepared under conditions of $w_{Cell}=$ 0.04 to 0.10 are listed in the third column of Table IV. Therefore, several hypothetical thin planes in the cast solution with a thickness of L_0 yield a new single hypothetical gel plane in the wet membrane (step i in Figure 10), and

Table III. Various kinds of porosity

Type	Notation	Definition	Eq	Ref
Volume fraction of polymer-lean phase in a hypothetical layer at the moment of phase separation	$Pr(\mathrm{PS})$ $(\equiv L)$	$\dfrac{R}{R+1}$	eq 36	—
Porosity of gel membrane after collapse of k layers	$Pr(\mathrm{GEL})$ $(\equiv L_A)$	$\left(\dfrac{R}{R+1}\right)^k$	eq 37	—
Porosity of dry membrane	$Pr(\mathrm{d}_1)$	$\left\{1-\left(\dfrac{S_2'}{S_2}\right)^3\right\}(1-L_A)+L_A$	eq 41	—
Porosity of dry membrane	$Pr(\mathrm{d}_2)$	$\pi N_P \bar{r}^2$	eq 50	4
Porosity of dry membrane	$Pr(\mathrm{d}_2)'$	$\pi\{N_{P(v)}\bar{r}^2+N_{P(i)}r(\mathrm{i})^2\}$	eq 52	—
Porosity of dry membrane evaluated from apparent density	$Pr(\mathrm{d}_3)$	$1-\dfrac{d_A}{d_{PL}}$	eq 42a	—
Porosity of dry membrane	$Pr(\mathrm{d}_3)'$	$1-\dfrac{d_A}{d_P'}$	eq 42b	—
Porosity of dry membrane determined by studying EM	$Pr(\mathrm{d}_4)(\equiv Pr(\mathrm{EM}))$	$\dfrac{\sum_i L_{C,i}}{\sum_i L_i}$	eq 43	8

Table IV. Characteristics of actual membranes and condition of theoretical calculations of pore radius distribution for these membranes

	Characteristics of actural membranes				Condition of theoretical calculation[b]			
w_{Cell}[a]	S_2'[c] / nm	k'[d]	$Pr(\mathrm{d}_3)$[e]	$Pr(\mathrm{d}_4)$[f]	d_P'[g] / $10^{-3}\,\mathrm{kg\,m^{-3}}$	$v_{p(2)}$[h]	S_2[i] / nm	R_A[h]
0.04	379	10.02	0.823	0.758	(1.10)	(0.731)	(379.4)	(3.12)
0.05	260	9.40	0.778	0.378	0.535	0.353	260.8	0.592
0.06	159	8.58	0.742	0.282	0.539	0.354	159.7	0.374
0.07	173	7.46	0.731	0.330	0.602	0.397	173.7	0.476
0.08	170	7.41	0.695	0.321	0.674	0.444	170.7	0.455
0.09	151	7.05	0.654	0.294	0.735	0.484	151.7	0.398
0.10	119	7.33	0.571	0.295	0.913	0.601	119.5	0.400

[a] Weight fraction of cellulose in cellulose cuprammonium solution; coagulating solution, $w_{Acetone}:w_{NH_3}:w_{H_2O}=0.30:0.0056:0.6944$; 298.15 K.
[b] $d_{PL}=1.5\times10^3\,\mathrm{kg\,m^{-3}}$; $Pr(\mathrm{d}_1)=Pr(\mathrm{d}_2)'=Pr(\mathrm{d}_3)'=Pr(\mathrm{d}_4)$; values with parentheses at $w_{Cell}=0.04$, not adopted in calculations.
[c] Scanning electron microscopic observation.
[d] Equation 55.
[e] Apparent density method (eq 42a).
[f] Equation 43.
[g] Equation 44.
[h] Equation 53.
[i] Equation 13.

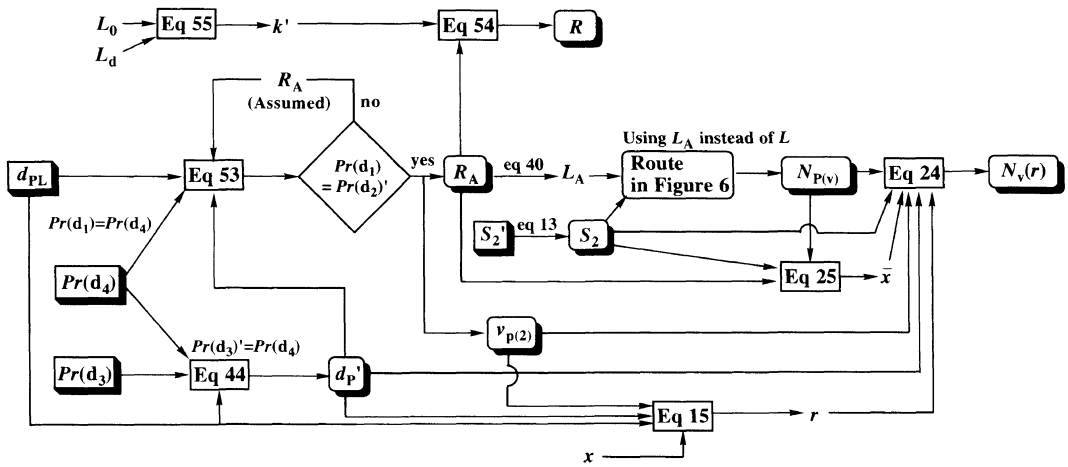

Figure 14. Route of calculation of R_A, S_2, d_P', $v_{p(2)}$, and pore size distribution for vacant-particle pores $N_v(r)$ from S_2', $Pr(d_3)$, and $Pr(d_4)$ evaluated by experiments and d_{PL}.

the new hypothetical planes contract again to give a dry membrane with a thickness of around a few tenth of L_0 (step h in Figure 10). In other words, even if we cut off a very thin plane with thickness of $2S_2'$ from the bulk dry membrane, the thin plane can never be regarded as a hypothetical plane, in which the phase separation occurred simultaneously under the same conditions.

Comparison of Theory with Experiment

The theory enables us to predict pore characteristics of membranes on the basis of knowledge on R_A (eq 53), S_2 (eq 13), d_P' (eq 44), and $v_{p(2)}$ (eq 53) under given casting conditions. Table IV collects S_2', $Pr(d_3)$, and $Pr(d_4)$ for membranes prepared under conditions of $w_{Cell}=0.04$ to 0.10. By using these values, d_P' was obtained by eq 44 and $v_{p(2)}$ and R_A were determined by eq 53 as summarized in the table. Route of calculation of R_A, S_2, d_P', and $v_{p(2)}$ and $N_v(r)$ is illustrated in Figure 14.

With an increase in w_{Cell}, both $Pr(d_3)$ and $Pr(d_4)$ decreased as expected. Under these preparative conditions, S_2' decreased with an increase in w_{Cell}. Except for $w_{Cell}=0.04$, d_P' and $v_{p(2)}$ were found to increase from 0.535 to 0.910, and 0.353 to 0.601, respectively with an increase in w_{Cell}. d_P' for $w_{Cell}=0.04$ was 1.10, which did not agree with a tendency observed in cases of w_{Cell} above 0.05, *i.e.*, the lower w_{Cell} is, the larger d_P' is. The disparity in d_P' at $w_{Cell}=0.04$ was caused by large $Pr(d_4)$. When w_{Cell} is lower, R becomes larger and accordingly, R_A is also larger. In a case of $w_{Cell}=0.04$, a part of polymer particles on the surface layer of a membrane can't connect to make a whole body of a network-like structure of the membrane because of larger R_A, *i.e.*, Pr(GEL). Omission of those unconnected polymer particles from the surface layer of the membrane occurs during washing process, resulting in an enlargement of $Pr(d_4)$. With an increase in cellulose concentration, R_A decreases gradually and is nearly 1/15 of R because of the collapse of gel layers.

R, calculated from R_A and k' by eq 54 (see, Figure 14) at $w_{Cell}=0.05$ to 0.10 as well as R, directly determined by phase equilibria experiments under the same conditions as those of casting at $w_{Cell}=0.04$, 0.05, and 0.08 are plotted in Figure 15. In the figure, closed and open circles are calculated and experimental data (R_{max}), respectively. Both R_s coincide well and this fact confirms that an effect of collapse during casting process on porosity of a membrane can be reasonably expressed by eq 37.

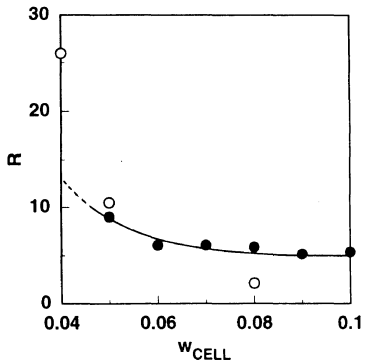

Figure 15. Comparison of R_{max}, evaluated by phase equilibria experiments under the same conditions with those of casting of cuprammonium cellulose membranes with R by eq 54 from R_A and k' data: Open circle, R_{max} by actual phase separation experiment; cellulose cuprammonium solution/acetone–water solution system; 298.15 K; closed circle, R by calculation; values of k', $Pr(d_3)$, $Pr(d_4)$, d_p', $v_{p(2)}$, and R_A as listed in Table IV are used; $Pr(d_1)=Pr(d_2)'=Pr(d_3)'=Pr(d_4)$.

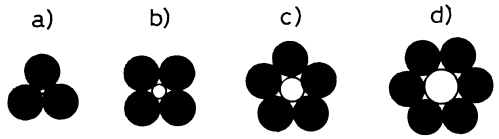

Figure 16. Schematic representation of an inter-polymer-particle pore, a lattice defect and a vacant-particle pore: a), Inter-polymer-particle pore, whose radius is $r_{(i)}$ (eq 33); b), Lattice defect as crevasse made by simultaneous contact of four polymer particles; c), Lattice defect as crevasse made by simultaneous contact of five polymer particles; d), Vacant-particle pore, whose radius is r_{min} (eq 16).

In this paper, all the pores whose pore radii are smaller than r_{min} (eq 16) are regarded as inter-polymer-particle pore which is illustrated in Figure 2d or in Figure 16a. $N(r)$ for inter-polymer-particle pores, $N_i(r)$ is given by the δ-function as eq 34. In an actual membrane there are a lot of small pores whose radii are smaller than r_{min} and in fact $N(r)$ by EM method[5] ($N(r)_{EM}$) has a large peak at r between 0 and r_{min}. By introducing the concept of the lattice defect as demonstrated in Figures 16b and 16c, we can improve a theory of $N(r)$ applicable only for vacant-particle pores ($r \geq r_{min}$). Instead, we can rewrite eq 34 in the zero-th approximation as:

$$N_i(r)=\frac{N_{P(i)}\delta(r-r_{(i)})}{r_{min}-r_{(i)}} . \quad (56)$$

Therefore, theoretical $N(r)$ is given as the summation of $N_v(r)$ and $N_i(r)$:

$$N(r)=N_v(r)+N_i(r) . \quad (57)$$

Here, note that $N_v(r)$ is never overlapped with $N_i(r)$ and we can not always count the number of all inter-polymer-particle pores and even some vacant-particle pores experimentally. Then, $N(r)_{EM}$ is expected of course less than theoretical $N(r)$.

Figures 17 shows the pore size distribution $N_v(r)$ (full line), calculated by eq 24 using the experimented data in Table IV on d_P', $v_{p(2)}$, S_2, and R_A, and $N_i(r)$ by eq 56 for membranes prepared under the conditions of $w_{Cell}=0.05$ to 0.10. In the figures, $N(r)_{EM}$ is also shown by open circles. In the range of *ca.* 0.1 μm$<r<$ *ca.* 0.5 μm, $N(r)_{EM}$ is slightly smaller than $N(r)$ and interestingly, in the range of $r<$ 0.1 μm, $N_i(r)$ point (closed circle) lies on the lines extrapolated or interpolated by $N(r)_{EM}$. Figure 17 means that some portion of vacant-particle pores whose r is in the range of 0.1 to 0.5 μm can not be accurately counted by EM.

CONCLUSIONS

(1) Theoretical equations are derived to express the pore size distribution $N(r)$ of vacant-particle pores constituted from vacant particles and inter-polymer-particle pores as crevasses between polymer particles for porous polymeric membranes prepared by the phase separation method.

(2) Pore density for vacant-particle pores N_P can be determined by the theory from two-phase volume ratio R and radius of polymer particles S_2 and thus $N(r)$ is obtained.

(3) As phase separation proceeds in an actual membrane, thickness of a gel membrane decreases, and particle density within a plane increases, resulting in an apparent increase in

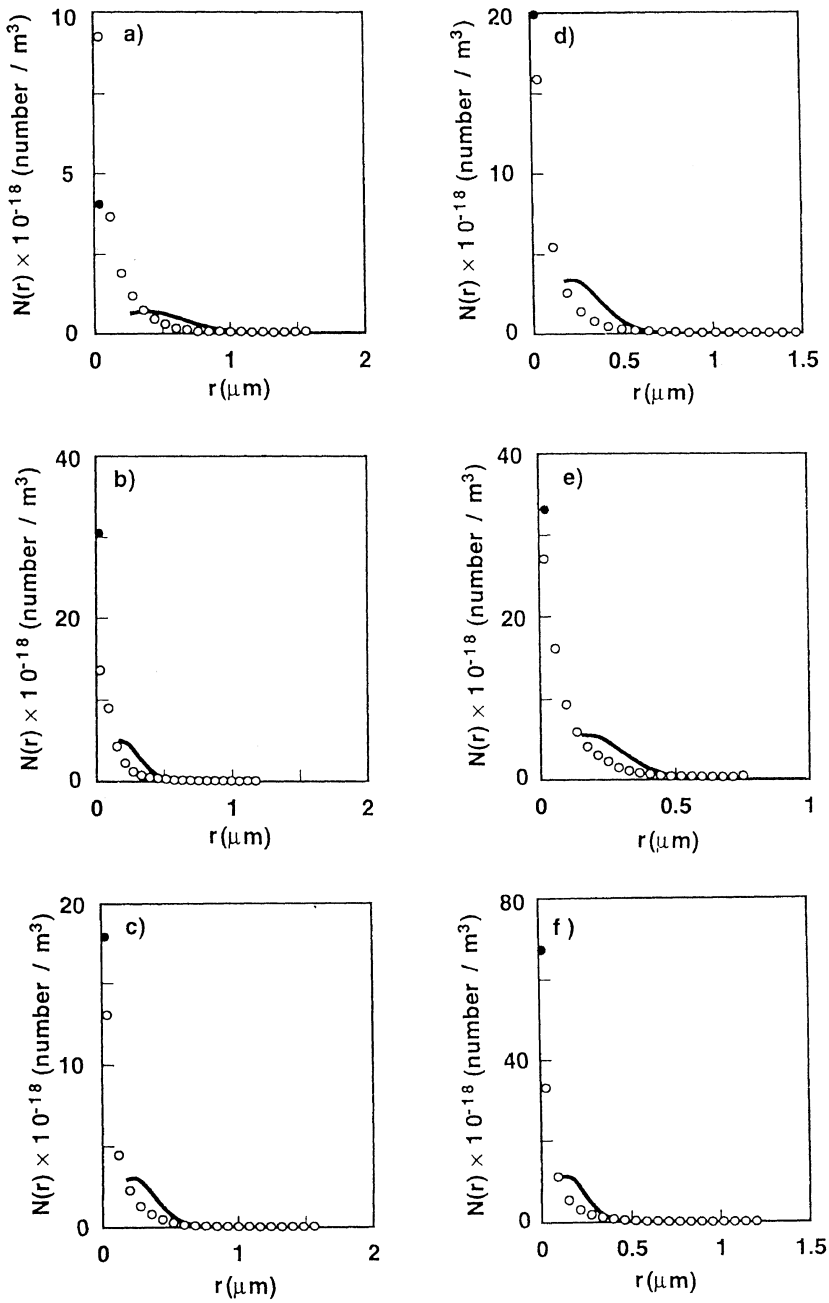

Figure 17. Comparison of experimental pore radius distribution $N(r)$ as determined by EM method with theoretical $N(r)$: open circle, EM method; full line, $N_v(r)$ (theoretical $N(r)$ for vacant-particle pores; eq 24); closed circle; $N_i(r)$ (theoretical $N(r)$ for inter-polymer-particle pore; eq 56); values of d_p', $v_{P(2)}$, S_2, and R_A listed in Table IV are employed; d_{PL}, 1.5×10^3 kg m^{-3}; a), w_{Cell}, 0.05; $N_{P(v)}$, 3.80×10^{11} number m^{-2}; b), w_{Cell}, 0.06; $N_{P(v)}$, 1.17×10^{12} number m^{-2}; c), w_{Cell}, 0.07; $N_{P(v)}$, 9.38×10^{11} number m^{-2}; d), w_{Cell}, 0.08; $N_{P(v)}$, 9.83×10^{11} number m^{-2}; e), w_{Cell}, 0.09; $N_{P(v)}$, 1.28×10^{12} number m^{-2}; f), w_{Cell}, 0.10; $N_{P(v)}$, 2.06×10^{12} number m^{-2}.

R to R_A.

(4) The pore size distribution $N(r)_s$ estimated by EM method were in good agreement with those by the theoretical calculation using R_A. We can design or predict pore characteristics of a membrane through use of this theory together with R_A and S_2.

APPENDIX I

Derivation of Equation 3

To find the number of distinguishable arrangements of partitioning balls into boxes, consider the following picture of the 4 balls in the 6 boxes.[19]

	|	○	|		|	○○	|		|	○	|		|
Box number:		1		2		3		4		5		6
Number of balls:		1		0		2		0		1		0

The lines mean the sides of the boxes and the open circles are the balls; note that it requires 7 lines to picture the 6 boxes. This picture shows one of many possible arrangements of the 4 balls in 6 boxes. In any such picture there must be a line at the beginning and at the end, but the rest of the lines (5 of them) and the 4 circles can be arranged in any order. Every arrangement of the balls in the boxes can be so pictured. Then the number of ways of partitioning 4 balls into 6 boxes, $W_6(4)$ is the number of ways we can select 4 positions for the 4 circles out of 9 positions for 5 lines and 4 circles, ${}_9C_4$.

In general, the number of ways, $W_b(a)$ of partitioning a balls into b boxes is given by the relation[19,20]

$$W_b(a) = {}_{\{(b-1)+a\}}C_a = \frac{\{(b-1)+a\}!}{(b-1)!a!}. \quad \text{(A-1)}$$

Note that some boxes may obtain no balls.

When we distribute 10 balls in 6 boxes on condition that each box has at least one ball, the number of such arrangement is just the number of ways of partitioning 4 balls in 6 boxes, $W_6(4)$.

Number of balls distributed beforehand:	|	○	|	○	|	○	|	○	|	○	|	○	|
Box number:		1		2		3		4		5		6
Number of balls partitioned later:	|	○	|		|	○○	|		|	○	|		|
Total number of balls in the boxes:	|	2	|	1	|	3	|	1	|	2	|	1	|

When we distribute N_TL vacant particles into N_P vacant-particle pores, each vacant-particle pore must have at least one vacant particle. Accordingly, the number of ways of partitioning N_TL vacant particles in N_P vacant-particle pores on condition that each pore has at least one vacant particle is just the number of ways of partitioning (N_TL-N_P) balls in N_P boxes, $W_{N_P}(N_TL-N_P)$, that is,

$$W_{N_P}(N_TL-N_P) = {}_{\{(N_P-1)+(N_TL-N_P)\}}C_{(N_TL-N_P)} = \frac{\{(N_P-1)+(N_TL-N_P)\}!}{(N_P-1)!(N_TL-N_P)!}. \quad \text{(A-2)}$$

APPENDIX II

Example of Calculating $P(x)$ by Using Equation 5

Consider a case of partitioning 5 vacant particles into 3 vacant-particle pores. After distributing one vacant particle to each pore, we can partition the remaining 2 vacant particles into 3 pores in the ways of $W_3(2)=6$:

(1)	|	○○○	|	○	|	○	|
(2)	|	○	|	○○○	|	○	|
(3)	|	○	|	○	|	○○○	|
(4)	|	○○	|	○○	|	○	|
(5)	|	○	|	○○	|	○○	|
(6)	|	○○	|	○	|	○○	|

Accordingly, the probability of appearance of the vacant-particle pores with one vacant particle, $P(1)$ is 9/18, *i.e.*, 1/2, and $P(1)$ value calculated by using eq 5 is $W_2(2)/W_3(2)=1/2$.

On the same ways, $P(2)$ and $P(3)$ can be also calculated by the equation as $W_2(1)/W_3(2)=1/3$ $(=6/18)$ and $W_2(0)/W_3(2)=1/6$ $(=3/18)$, respectively.

APPENDIX III

Derivation of Equation 6

Dividing both numerator and denominator of eq 5 by N_TL, we have

$$P(x)=\frac{(N_TL-N_P)(N_TL-N_P-1)\cdots(N_TL-N_P-x+2)(N_P-1)}{(N_TL-1)(N_TL-2)\cdots(N_TL-x)}$$
$$=\frac{\left(1-\frac{N_P}{N_TL}\right)\left(1-\frac{N_P}{N_TL}-\frac{1}{N_TL}\right)\cdots\left\{1-\frac{N_P}{N_TL}-\frac{(x-2)}{N_TL}\right\}\left(\frac{N_P}{N_TL}-\frac{1}{N_TL}\right)}{\left(1-\frac{1}{N_TL}\right)\left(1-\frac{2}{N_TL}\right)\cdots\left(1-\frac{x}{N_TL}\right)}. \quad \text{(A-3)}$$

If $N_TL \gg x$ and $N_P < N_TL$, $P(x)$ can be simplified into

$$P(x)\cong\frac{\left(1-\frac{N_P}{N_TL}\right)^x\left(\frac{N_P}{N_TL}\right)}{\left(1-\frac{N_P}{N_TL}\right)}\cong\frac{\left(1-\frac{N_P}{N_TL}\right)^x}{\left(\frac{N_TL}{N_P}-1\right)}. \quad (6)$$

GLOSSARY OF SYMBOLS

L	volume fraction of polymer-lean phase
L_0	thickness of cast solution
L_A	apparent volume fraction of polymer-lean phase
$L_{C,i}$	cut-off length, by pores, of the i-th test line
L_d	thickness of dry membrane
L_g	thickness of a coagulated gel membrane
L_i	length of the i-th test lines drawn on a photograph of membrane surface
$N_i(r)$	pore size distribution for inter-polymer-particle pores
N_P	number of vacant-particle pores in unit area of a membrane (=pore density)
$N_{P(i)}$	number of inter-polymer-particle pores in unit area of a membrane
$N_{P(v)}$	N_P theoretically expected for a given combination of R and S_2 under the random distribution of particles; N_P value which satisfies eq 28
$N'_{P,peak}$	Upper limit of N_P in a case when $N(r)$ has a peak at $r>r_{min}$
$N(r)$	pore size distribution
$N(r)_{EM}$	$N(r)$ experimentally determined by the electron micrographic method
N_T	total number of polymer- and vacant-particles in unit area of a plane
$N_v(r)$	$N(r)$ for vacant-particle pore
$N_v(r_{peak})$	value of $N_v(r)$ at $r=r_{peak}$
$N^*(r^*)$	$=N_v(r)S_2/2N_{P(v)}$
$P_n(m)$	probability that a given polymer particle is surrounded in part by m vacant particles, which belong to n different pores
Pr	porosity of a membrane
$Pr(d_1)$	porosity of dry membrane
$Pr(d_2)$	porosity of dry membrane
$Pr(d_2)'$	porosity of dry membrane
$Pr(d_3)$	porosity determined by the apparent density method
$Pr(d_3)'$	real porosity of dry membrane
$Pr(d_4)$	porosity of dry membrane determined from electron micrographs
Pr(GEL)	volume fraction of vacant particles in a gel membrane
Pr(PS)	volume fraction of a polymer-lean phase in a hypothetical layer at the

	moment of phase separation
$P(x)$	probability of appearance of the vacant-particle pore with x vacant particles
R	two-phase volume ratio ($\equiv V_{(1)}/V_{(2)}$)
R_A	apparent phase volume ratio
R_{max}	the largest R value experimentally obtained
R'_{peak}	Lower limit of R in a case when $N(r)$ has a peak at $r > r_{min}$
S_2	radius of wet polymer particle (=secondary particle)
S'_2	radius of dry polymer particle (=secondary particle)
$V_{(1)}$	volume of polymer-lean phase
$V_{(2)}$	volume of polymer-rich phase
$W_b(a)$	number of ways of partitioning a vacant particles into b cells
X_n	number-average degree of polymerization
X_w	weight-average degree of polymerization
d_A	apparent density of a membrane
d_P'	density of dried polymer particles
d_{PL}	density of polymer constructing a membrane
$f_H(x_H)$	minimum number of polymer particles needed to surround fully a regular hexagonal pore consisting of x_H vacant-particles
$f(x)$	minimum number of polymer particles needed to surround fully an assembly of x vacant particles
k	degree of collapse of a membrane; number of layers collapsed during coagulation step ($\cong L_0/L_g$)
k'	approximate of k' ($=L_0/L_d$)
m	number of the nearest neighbor vacant particles existing around a given polymer particle
n	number of vacant-particle pores which a given single polymer particle is directly participated to form ($1 \leq n \leq 3$)
$1/n$	reciprocal n; contribution fraction of one polymer particle to the formation of one vacant-particle pore
$\overline{(1/n)}$	average contribution fraction of one polymer particle to the formation of one vacant-particle pore
$n_{(i)}$	number of inter-polymer-particle pores directly contacted with a given single polymer particle
$\overline{n_{(i)}}$	average number of inter-polymer-particle pores directly contacted with a given single polymer particle
p_1	1st order concentration-dependent parameter of thermodynamic interaction parameterxbetween solvent and polymer
r	pore radius of dry membrane
r_{Wet}	pore radius of wet gel membrane
$r_{(i)}$	radius of inter-polymer-particle pore of dry membrane
$r_{(i)Wet}$	radius of inter-polymer-particle pore of wet gel membrane
r_{min}	minimum of radius of vacant-particle pore consisting of a single vacant particle
r_{peak}	pore radius which gives a peak of $N_v(r)$
$\bar{r}$	average pore radius of dry membrane
r^*	$\equiv r/S_2$
v_m	volume of absolutely dry membrane
v_p^0	polymer volume fraction of solution when phase separation occurs
$v_{p(2)}$	polymer volume fraction of polymer rich-phase in equilibrium
v_p^c	polymer volume fraction at a critical solution point
$w_{Acetone}$	weight fraction of acetone
w_{Cell}	weight fraction of cellulose
w_{Cu}	weight fraction of copper
w_{H_2O}	weight fraction of water
w_{NH_3}	weight fraction of ammonia
w_m	weight of absolutely dry membrane
x	number of vacant particles constituting a single vacant-particle pore on the hexagonal lattice sites

x_H number of vacant particles constituting a regular hexagonal vacant-particle pore on the hexagonal lattice sites

$\bar{x}$ average x

χ_{12}^0 thermodynamics interaction parameter between solvent and nonsolvent

χ_{13}^0 thermodynamics interaction parameter between solvent and polymer

χ_{23}^0 thermodynamics interaction parameter between nonsolvent and polymer

$\delta(r)$ δ-function

ρ_p relative amount of polymer precipitated

Acknowledgment. The authors express their sincere gratitude to Miss Miki Inamoto of Fundamental Research Laboratory of Natural & Synthetic Polymers, Asahi Chemical Industry Co., Ltd. for her technical assistance in EM measurements.

REFERENCES

1. K. Kamide, H. Iijima, and S. Matsuda, *Polym. J.*, **25**, 1113 (1993).
2. K. Kamide, H. Iijima, and H. Shirataki, *Polym. J.*, **26**, 21 (1994).
3. K. Kamide, S. Manabe, T. Matsui, T. Sakamoto, and S. Kajita, Koubunshi Ronbunshu, **34**, 205 (1977).
4. K. Kamide and S. Manabe in "Materials Science of Synthetic Membranes," D. R. Lloyd, Ed., ACS Symposium Series, No. 269, American Chemical Society, Washington, D.C., 1985, p 197.
5. S. Manabe, Y. Shigemoto, and K. Kamide, *Polym. J.*, **17**, 775 (1985).
6. S. Manabe, Y. Kamata, H. Iijima, and K. Kamide, *Polym. J.*, **19**, 391 (1987).
7. S. Manabe, H. Iijima, and K. Kamide, *Polym. J.*, **20**, 307 (1988).
8. K. Kamide and S. Manabe in "Ultrafiltration Membranes and Applications," Polymer Science and Technology, Vol. 13, A. R. Cooper, Ed., Plenum Press, New York, N. Y., 1980, pp 173–202.
9. K. Kamide and K. Sugamiya, *Macromol. Chem.*, **139**, 197 (1970).
10. K. Kamide and K. Sugamiya, *Macromol. Chem.*, **156**, 259 (1972).
11. K. Kamide, Y. Miyazaki, and K. Sugamiya, *Macromol. Chem.*, **173**, 113 (1973).
12. K. Kamide, K. Yamaguchi, and Y. Miyazaki, *Macromol. Chem.*, **173**, 133 (1973).
13. K. Kamide and Y. Miyazaki, *Macromol. Chem.*, **176**, 1029 (1975).
14. K. Kamide and Y. Miyazaki, *Macromol. Chem.*, **176**, 1051 (1975).
15. K. Kamide, Y. Miyazaki, and T. Abe, *Macromol. Chem.*, **177**, 485 (1976).
16. K. Kamide, S. Matsuda, and Y. Miyazaki, *Polym. J.*, **16**, 479 (1984).
17. K. Kamide and S. Matsuda, *Polym. J.*, **16**, 515 (1984).
18. K. Kamide and S. Matsuda, *Polym. J.*, **16**, 591 (1984).
19. M. L. Boas, "Mathematical Methods in the Physical Science," John Wiley & Sons, Inc., New York, N. Y., 1966, p 693.
20. R. Kubo, "Statistical Mechanics–An advanced Course with Problems and Solutions," North-Holland Publishing Co., Amsterdam, The Netherlands, 1965, p 36.